Computers and Mathematics with Applications 64 (2012) 1441–1449

Contents lists available at SciVerse ScienceDirect

Computers and Mathematics with Applications

journal homepage: www.elsevier.com/locate/camwa

Using a particle swarm method to optimize the weighting in extension theory for the detection of islanding in photovoltaic systems

Uei-Dar Lai, Kuei-Hsiang Chao *, Meng-Hui Wang

Department of Electrical Engineering, National Chin-Yi University of Technology, Taichung 41107, Taiwan

ARTICLE INFO

Keywords:
Two-dimensional particle swarm optimization (2D-PSO)
Extension theory
Islanding detection
Photovoltaic (PV) power generation system

ABSTRACT

This paper proposes a two-dimensional particle swarm optimization (2D-PSO) method for optimizing the weighting in extension theory for the detection of islanding in photovoltaic (PV) power generation systems. Generally, using extension theory to implement and analyze a system with a correlation function would involve constructing a weighting determined by trial and error to help judge the problem's performance. However, the judgment accuracy can be degraded if one uses an inappropriate weighting set. Hence, this paper proposes a weighting determination method for optimizing the performance of the extension method using the 2D-PSO algorithm. Some simulation results are obtained to verify the effectiveness of the proposed islanding detection method. In addition, the simulated results obtained using the proposed 2D-PSO algorithm are also compared with those obtained using genetic algorithm (GA) and evolutionary programming (EP) algorithms in order to reveal the search performance of the proposed method.

1. Introduction

Islanding detection is a significant PV technique as regards protecting personnel, avoiding equipment damage and maintaining power quality in power systems. There are two classifications of islanding detection techniques: those including passive [1–4] and active detection modes [5–8]. The main passive detection techniques are the voltage phase jump detection method, the frequency changing rate detection method and the detection method based on the third-harmonic distortion of a voltage surge [1]. The main active detection techniques are the active voltage drift method [5], the active frequency drift method [6], the slip mode frequency drift method [7] and the load variation method [8]. A research approach adopting an extension theory based multi-variable method that combines passive and active detection methods to detect an islanding problem in PV power generation systems was introduced in [9]. However, it used a trial-and-error weighting in the extension engineering method to identify seven islanding phenomena: voltage swell, voltage dip, injected harmonic power, normal operation, islanding operation below or above the normal operation limitations and voltage flicker. The trial-and-error weighting method might lead to a wrong judgment problem when dealing with some critical cases.

The evolutionary genetic algorithms (GA) [10,11] and evolutionary programming (EP) [11] algorithms are search algorithms based on the simulated evolutionary process of natural selection, variation, and genetics. The evolutionary algorithms are more flexible and robust than conventional trial-and-error methods. Although a GA approach can provide a near global solution, the encoding and decoding schemes means that it takes a longer time to achieve convergence. However, an EP algorithm uses the control parameters [11], but not their coding, as in the GA approach. In addition, the EP algorithm relies primarily on mutation and selection, but not crossover, as in the GA approach. Hence, considerable computation time may be saved by using an EP algorithm. Although GA and EP algorithms seem to be good methods for solving optimization

* Corresponding author. Tel.: +886 423924505x7272; fax: +886 423922156.
E-mail address: chaokh@ncut.edu.tw (K.-H. Chao).

0898-1221/$ – see front matter © 2012 Elsevier Ltd. All rights reserved.
doi:10.1016/j.camwa.2012.03.091

problems, when applied to problems consisting of greater numbers of local minima, the solutions obtained from both methods are just ones near the global optimum ones [11]. Additionally, GA and EP algorithms take long computation times to obtain the solutions for such problems [11]. Like other evolutionary algorithms, the particle swarm optimization (PSO) algorithm starts with random initialization of a population of individuals in the search space [12–16]. However, unlike in other evolutionary algorithms, in PSO there is no direct recombination of genetic material between individuals during the search process. The PSO works on the social behavior of particles in the swarm. Therefore, it finds the global optimum solution by simply adjusting the trajectory of each individual toward its own best location and toward the best particle of the entire swarm at each step. The PSO method is a stochastic search technique with simplicity of implementation and the ability to more quickly converge to a reasonably good solution as compared to other evolutionary algorithms.

On the basis of the above, a 2D-PSO method is proposed in this paper for searching for the optimal weighting in an existing extension islanding detection method [9] for a PV power generation system. Through enlarging the correlation degree difference between two adjacent islanding types, the judgment accuracy of islanding detections can be promoted for a PV generation system.

2. A summary of particle swarm optimization

Particle swarm optimization (PSO) is a stochastic optimization technique developed by Eberhart and Kennedy in 1995, inspired by the social behavior of bird flocking or fish schooling [12]. A kernel concept for the optimization of nonlinear functions using particle swarm methodology is introduced in [13].

The general PSO algorithm first defines the potential solutions, called particles, then moves each of the particles to the next position according to a velocity function, and finally checks whether these potential particles can approach the globally best solution or exactly find it [14]. The following is a pseudo-code for the procedure used to implement the proposed 2D-PSO algorithm:

2D-PSO procedure
{
Define particle numbers (N) and maximum iteration number (i_max);
Initialize all particles' positions (px_j, py_j) and velocities (vx_j, vy_j);
Define all particles' best locations (bx_j, by_j) as (px_j, py_j);
Define the global best position (Gx, Gy) and initialize as (0, 0);
For $i = 1$ to i_max {
  For $j = 1$ to N {
    Calculate the new velocity and position of each particle:
      $(vx_{j+1}, vy_{j+1}) = \text{velocity}(vx_j, vy_j, bx_j, by_j, px_j, py_j, Gx, Gy)$;
      $(px_{j+1}, py_{j+1}) = (vx_{j+1}, vy_{j+1}) + (px_j, py_j)$;
    Calculate the fitness values:
      New performance = fitness (x_{j+1}, y_{j+1});
      Current best performance = fitness $((px_j, py_j))$;
    Upgrade each particle's best position:
      If (New performance) > (Current best performance)
      Then $(bx_j, by_j) = (px_{j+1}, py_{j+1})$;
    }
  Get the best position (x_{best}, y_{best}) from all the particles;
  Update global best positions:
    If fitness (x_{best}, y_{best})> fitness (Gx, Gy),
    Then $(Gx, Gy) = (x_{best}, y_{best})$;
  Record new positions and velocities of all particles;
  }
}

where the velocity function uses the following two formulas:

$$vx_{j+1} = w^* vx_j + \eta 1^* rand(1)^* (bx_j - px_j) + \eta 2^* rand(1)^* (Gx - px_j)$$
$$vy_{j+1} = w^* vy_j + \eta 1^* rand(1)^* (by_j - py_j) + \eta 2^* rand(1)^* (Gy - py_j)$$

where $\eta 1$, $\eta 2$ are positive learning factors, w is an inertia weight and $rand(1)$ is a random value from 0 to 1; the fitness function is the user-defined function for reaching the best performance.

The fitness function in the 2D-PSO procedure is based on the input of two random weight numbers into the correlation function of the extension method and then feedback of the result from the fitness subroutine. The running continues for

Table 1
The matter-element model for islanding detection.

Category	Classical field
I_1	$R_1 = \begin{bmatrix} F_0 & c_1, & \langle 327{,}560\rangle \\ & c_2, & \langle 59.5, 60.4\rangle \\ & c_3, & \langle -31.65, 45\rangle \end{bmatrix}$
I_2	$R_2 = \begin{bmatrix} F_0 & c_1, & \langle 125, 280.805\rangle \\ & c_2, & \langle 59.1, 60.8026\rangle \\ & c_3, & \langle -30, 20\rangle \end{bmatrix}$
I_3	$R_3 = \begin{bmatrix} F_0 & c_1, & \langle 276.5, 295\rangle \\ & c_2, & \langle 59.6, 60.2\rangle \\ & c_3, & \langle -165, -1\rangle \end{bmatrix}$
I_4	$R_4 = \begin{bmatrix} F_0 & c_1, & \langle 309, 313.5\rangle \\ & c_2, & \langle 59.3, 60.5\rangle \\ & c_3, & \langle -20.7, 1\rangle \end{bmatrix}$
I_5	$R_5 = \begin{bmatrix} F_0 & c_1, & \langle 566,\ 680\rangle \\ & c_2, & \langle 58.9, 90\rangle \\ & c_3, & \langle -21.54, -14\rangle \end{bmatrix}$
I_6	$R_6 = \begin{bmatrix} F_0 & c_1, & \langle 1,\ 250\rangle \\ & c_2, & \langle -65, 65\rangle \\ & c_3, & \langle -190, 5\rangle \end{bmatrix}$
I_7	$R_7 = \begin{bmatrix} F_0 & c_1, & \langle 298,\ 320.5\rangle \\ & c_2, & \langle 58.785, 59.98\rangle \\ & c_3, & \langle -145,\ 85\rangle \end{bmatrix}$

all of the particles until the maximum iteration number is reached, and it is checked whether the global best result could match the target of better weighting.

3. A summary of the extension theory

The extension theory was created by Wen Cai in 1983 and developed in order to solve the complicated and contradictory problems encountered in human life [17]. The first concept of the theory is that all matter in the world can be described using a matter-element model $R = (N, C, V)$. R is called a matter-element, N is the name of R, C is a characteristic vector of N and V is the magnitude vector of C. The application of extension theory in the engineering field is called the extension engineering method [18].

Fig. 1 shows the architecture of the proposed 2D-PSO algorithm based on extension theory for islanding detection, which contains a power conditioner, an *LC*-filter, an intelligent islanding detection controller, a grid power, and an *RLC* parallel load. Within the architecture, V_{dc} is the output voltage of a photovoltaic module. Following [9], seven categories were created and these are shown in Table 1.

The islanding characteristics are selected as the peak voltage (c_1), frequency (c_2) and phase difference (c_3). The following are the steps of the extension method used to build up the matter-element model and identify the islanding category.

Step (1). Create the entire matter-element model for the analyzed islanding problem. In Table 1 the classical field V_{pk} for each characteristic is the category range that the classical sample's characteristic for the category should be located in. Meanwhile, create a joint field V_{qn} that contains the overall ranges of all classical fields in every characteristic.

$$R_p = (F_0, C, V_p) = \begin{bmatrix} F_0, & c_1, & V_{p1} \\ & c_2, & V_{p2} \\ & \vdots & \vdots \\ & c_k, & V_{pk} \end{bmatrix} = \begin{bmatrix} F_0, & c_1, & \langle a_{p1}, b_{p1}\rangle \\ & c_2, & \langle a_{p2}, b_{p2}\rangle \\ & \vdots & \vdots \\ & c_k, & \langle a_{pk}, b_{pk}\rangle \end{bmatrix} \tag{1}$$

where $V_{pk} = \langle a_{pk}, b_{pk}\rangle_{k=1,2,3}$ is the classical field for each characteristic of every islanding category shown in Table 1.

The representative symbols of these operation categories are described below.

I_1: Voltage swell

I_2: Voltage dip

I_3: Injected power harmonic

I_4: Normal operation

I_5: Islanding operation above normal operation limit

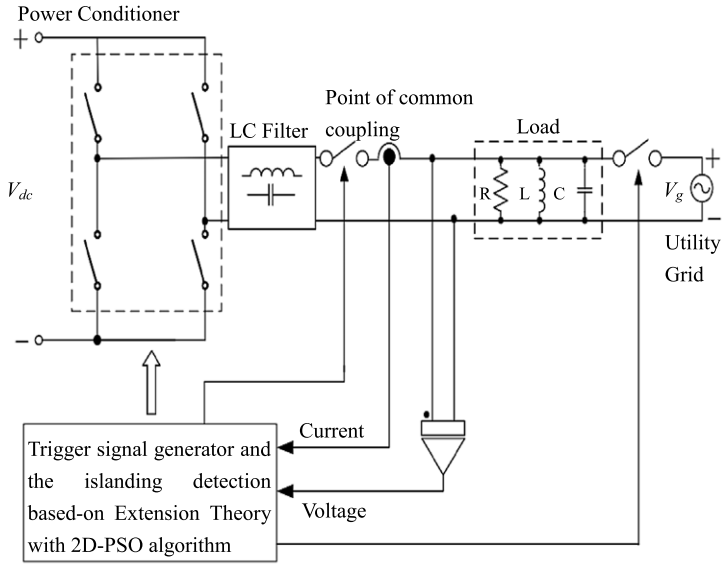

Fig. 1. Architecture of the proposed 2D-PSO based on extension theory for the islanding detection.

Table 2
The 14 tested data for islanding detection.

Test No.	1	2	3	4	5	6	7
Peak voltage (V)	387.96	290.879	349.99	273.324	217.699	609.599	217.699
Frequency (Hz)	59.683	60.24	60.009	59.77	60.009	60.009	59.98
Phase difference (deg)	−16.25	−157.306	−20.707	−92.653	−20.649	−19.612	−20.736
Islanding detection type	I_1	I_3	I_1	I_3	I_2	I_5	I_2
Test No.	8	9	10	11	12	13	14
Peak voltage (V)	311.101	138.17	615.778	305.491	311.106	3.428	313.768
Frequency (Hz)	59.98	60.009	59.98	59.665	59.98	60.009	60.009
Phase difference (deg)	−19.526	−20.649	−19.065	−20.131	−19.526	−45.014	−20.649
Islanding detection type	I_4	I_6	I_5	I_7	I_4	I_6	I_7

I_6: Islanding operation below normal operation limit

I_7: Voltage flicker

$$R_F = (F, C, V_q) = \begin{bmatrix} F, & c_1, & V_{q1} \\ & c_2, & V_{q2} \\ & c_3, & V_{q3} \end{bmatrix} = \begin{bmatrix} F & c_1, & \langle a_{q1}, b_{q1} \rangle \\ & c_2, & \langle a_{q2}, b_{q2} \rangle \\ & c_3, & \langle a_{q3}, b_{q3} \rangle \end{bmatrix} \tag{2}$$

where $V_{q1} = \langle 1, 680 \rangle$, $V_{q2} = \langle -65, 90 \rangle$ and $V_{q3} = \langle -190, 85 \rangle$ are the joint fields of each characteristic.

Step (2). Get a tested sample with a matter-element model for islanding detection.

$$R_m = \begin{bmatrix} F_m, & c_1, & v_1 \\ & c_2, & v_2 \\ & c_3, & v_3 \end{bmatrix}, \quad m = 1, 2, \ldots, 14 \tag{3}$$

where R_m is one of the tested samples in Table 2.

Step (3). Define a correlation function for calculating the correlation degrees for each characteristic and then assign the individual weight for each correlation degree to obtain the total correlation value λ_p. The correlation degree is "distance" divided by "rank value".

$$K(v_k) = \frac{\rho(v_k, F_0)}{D(v_k, F_0, F)}, \quad k = 1, 2, 3 \tag{4}$$

$$\rho(v, F_0) = \left| v - \frac{a_p + b_p}{2} \right| - \frac{b_p - a_p}{2} \tag{5}$$

Table 3
Detection result for islanding detection types based on $W_{p1} = 0.427$, $W_{p2} = 0.3$ and $W_{p3} = 0.273$.

Test No.	Correlation degrees with respect to each type							Known types	Detected results	1st max. (A)	2nd max. (B)	(A–B)
	I_1	I_2	I_3	I_4	I_5	I_6	I_7					
1	0.4551	0.2410	0.0307	0.2167	0.0163	−0.0530	0.3094	I_1	I_1	0.4551 (I_1)	0.3094 (I_7)	0.1457 (I_1–I_7)
2	−0.1573	−0.3333	0.2154	−0.1154	−0.4021	0.0607	−0.0875	I_3	I_3	0.2154 (I_3)	0.0607 (I_6)	0.1547 (I_3–I_6)
3	0.4229	0.3071	0.1956	0.2030	−0.0872	−0.0043	0.2156	I_1	I_1	0.4229 (I_1)	0.3071 (I_2)	0.1158 (I_1–I_2)
4	0.0045	0.1702	0.4059	0.0695	−0.3196	0.2630	0.1942	I_3	I_3	0.4059 (I_3)	0.2630 (I_6)	0.1429 (I_3–I_6)
5	0.1959	0.7277	0.1653	0.1202	−0.1773	0.2056	0.1351	I_2	I_2	0.7277 (I_2)	0.2056 (I_6)	0.5221 (I_2–I_6)
6	0.1701	0.0415	−0.0959	−0.0721	0.4873	−0.2651	−0.0953	I_5	I_5	0.4873 (I_5)	0.1701 (I_1)	0.3172 (I_5–I_1)
7	0.2146	0.7369	0.1946	0.1333	−0.1842	0.2060	0.1356	I_2	I_2	0.7369 (I_2)	0.2146 (I_1)	0.5223 (I_2–I_1)
8	0.3455	0.3663	0.2606	0.6883	−0.0260	0.0216	0.6049	I_4	I_4	0.6883 (I_4)	0.6049 (I_7)	0.0834 (I_4–I_7)
9	0.0917	0.4540	0.0420	0.0100	−0.2374	0.4784	0.0207	I_6	I_6	0.4784 (I_6)	0.4540 (I_2)	0.0244 (I_6–I_2)
10	0.1712	0.0510	−0.0756	−0.0510	0.5730	−0.2727	−0.1037	I_5	I_5	0.5730 (I_5)	0.1712 (I_1)	0.4018 (I_5–I_1)
11	0.1639	0.2749	0.1145	0.1920	−0.0801	0.0292	0.6921	I_7	I_7	0.6921 (I_7)	0.2749 (I_2)	0.4172 (I_7–I_2)
12	0.3455	0.3663	0.2606	0.6892	−0.0260	0.0216	0.6047	I_4	I_4	0.6892 (I_4)	0.6047 (I_7)	0.0845 (I_4–I_7)
13	−0.1886	−0.1672	−0.0857	−0.2211	−0.4455	0.1714	−0.1864	I_6	I_6	0.1714 (I_6)	−0.0857 (I_3)	0.2571 (I_6–I_3)
14	0.3217	0.3411	0.2322	0.2464	−0.1047	0.0225	0.5060	I_7	I_7	0.5060 (I_7)	0.3411 (I_2)	0.1649 (I_7–I_2)

$$D(v, F_0, F) = \begin{cases} \rho(v, F) - \rho(v, F_0) & \text{for } v \notin F_0 \\ -\dfrac{|a_p - b_p|}{2} & \text{for } v \in F_0 \end{cases} \tag{6}$$

$$\rho(v, F) = \left| v - \frac{a_q + b_q}{2} \right| - \frac{b_q - a_q}{2} \tag{7}$$

where $K(v_k)$ is called the "correlation degree", $\rho(v_k, F_0)$ is called the "distance" and $D(v_k, F_0, F)$ is called the "rank value". Calculating the test sample matter-element R_m with the appropriate "distance" and "rank value" to get the correlation degree K is the main calculation section of the extension method.

$$\lambda_p = \sum_{k=1}^{3} W_{pk} K_{pk}, \quad p = 1, 2, \ldots, 7 \tag{8}$$

where $W_{p3} = (1 - W_{p1} - W_{p2})$ and (W_{p1}, W_{p2}) are randomly obtained from the PSO subroutine.

Step (4). Select the maximal value of λ_p in order to recognize the right category of the islanding problem.

$$\text{If } (\lambda_p \text{is maximum}), \text{ then } (I_x = I_p). \tag{9}$$

Step (5). If a new tested sample exists, then go back to Step 2, or else end the procedure.

4. Simulation results

In this paper, Kyocera KC40T [19] photovoltaic modules are connected as a photovoltaic power system with a rated output voltage of 208 V (12 modules connected in series), a rated output current of 2.48 A, and a rated output power of 516 W. This PV power system combines the grid powers to form a grid-connected PV power system. Table 3 shows the simulation results obtained using a set trial-and-error weightings of $W_{p1} = 0.427$, $W_{p2} = 0.3$ and $W_{p3} = 0.273$; the key performance index of the weighting assignment is the difference between the first and the second maximum correlation values shown in the last column of the table, and the larger the difference is, the better. Another trial-and-error case, shown in Table 4, with $W_{p1} = 0.3$, $W_{p2} = 0.3$ and $W_{p3} = 0.4$ indicates that the tests Nos. 1, 8, 9 and 12 would involve wrong judgments. These phenomena of wrong judgment show how important the weighting assignment is.

In this paper, a fitness function representing the difference between the first and second maximum correlation values calculated using the extension method is defined as follows:

$$\text{Fitness function} = min\{\lambda_p - \lambda_q\} \geq d\lambda_{set} \tag{10}$$

where λ_p and λ_q are the first and second maximum correlation values calculated using the extension islanding detection algorithm, respectively. And $d\lambda_{set}$ is the expected correlation value difference between two adjacent islanding types. The simulation parameters of the proposed 2D-PSO algorithm for all the test cases are fixed as follows: learning factors $\eta 1 = \eta 2 = 1$, inertia weight $w = 0.8$, number of particles $N = 10$, maximum iteration number $i\_max = 100$, initial global best position $(Gx, Gy) = (1/3, 1/3)$ and $rand(1)$ is a random value from 0 to 1.

After using MATLAB to implement the proposed 2D-PSO algorithm and obtain the globally best weighting, the new islanding detection result obtained is that shown in Table 5. It is clear from Table 3 and Table 5, that the key performance index (the difference between the first and the second maximal correlation values) in the last column has been changed from 0.0244 to 0.1318. The value 0.1318 is large enough to separate the first and the second maximal correlation values of

Table 4
New detection result based on $W_{p1} = 0.3$, $W_{p2} = 0.3$ and $W_{p3} = 0.4$.

Test No.	Correlation degrees with respect to each type							Known types	Detected results	1st max. (A)	2nd max. (B)	(A–B)
	I_1	I_2	I_3	I_4	I_5	I_6	I_7					
1	0.4397	0.3449	0.0850	0.2946	0.1402	0.0155	0.4450	I_1	I_7	0.4550 (I_7)	0.4397 (I_1)	0.0053 (I_7–I_1)
2	−0.2440	−0.1301	0.1708	−0.2104	−0.4426	0.1190	−0.1192	I_3	I_3	0.1708 (I_3)	0.1190 (I_6)	0.0518 (I_3–I_6)
3	0.4341	0.3764	0.2443	0.2156	−0.0089	0.0587	0.3428	I_1	I_1	0.4341 (I_1)	0.3764 (I_2)	0.0577 (I_1–I_2)
4	−0.0235	0.1083	0.5195	0.0302	−0.3075	0.3998	0.2626	I_3	I_3	0.5195 (I_3)	0.3998 (I_6)	0.1197 (I_3–I_6)
5	0.2749	0.6723	0.2228	0.1585	−0.0690	0.2061	0.2861	I_2	I_2	0.6723 (I_2)	0.2861 (I_6)	0.3862 (I_2–I_6)
6	0.2624	0.1988	0.0367	0.0433	0.4552	−0.1268	0.1224	I_5	I_5	0.4552 (I_5)	0.2624 (I_1)	0.1928 (I_5–I_1)
7	0.2933	0.6811	0.2522	0.1709	−0.0788	0.2066	0.2867	I_2	I_2	0.6811 (I_2)	0.2933 (I_1)	0.3878 (I_2–I_1)
8	0.3919	0.4308	0.2956	0.5834	0.0992	0.0744	0.6142	I_4	I_7	0.6142 (I_7)	0.5834 (I_4)	0.0308 (I_7–I_4)
9	0.2017	0.4800	0.1362	0.0810	−0.1112	0.3977	0.2057	I_6	I_2	0.4800 (I_2)	0.3977 (I_6)	0.0823 (I_2–I_6)
10	0.2719	0.2131	0.0582	0.0728	0.5454	−0.1333	0.1156	I_5	I_5	0.5454 (I_5)	0.2719 (I_1)	0.2735 (I_5–I_1)
11	0.2104	0.3345	0.1483	0.2001	0.0259	0.0815	0.7236	I_7	I_7	0.7236 (I_7)	0.3345 (I_2)	0.3891 (I_7–I_2)
12	0.3919	0.4308	0.2956	0.5841	0.0992	0.0744	0.6141	I_4	I_7	0.6141 (I_7)	0.5841 (I_4)	0.0300 (I_7–I_4)
13	−0.0744	−0.0559	0.1083	−0.1152	−0.3385	0.2341	0.0499	I_6	I_6	0.2341 (I_6)	0.1083 (I_3)	0.1258 (I_6–I_3)
14	0.3633	0.4007	0.2699	0.2471	−0.0180	0.0775	0.5467	I_7	I_7	0.5467 (I_7)	0.4007 (I_2)	0.1460 (I_7–I_2)

Table 5
New detection result based on $W_{p1} = 0.531$, $W_{p2} = 0.273$ and $W_{p3} = 0.196$.

Test No.	Correlation degrees with respect to each type							Known types	Detected results	1st max. (A)	2nd max. (B)	(A–B)
	I_1	I_2	I_3	I_4	I_5	I_6	I_7					
1	0.4676	0.1522	−0.0162	0.1468	−0.0704	−0.1053	0.2086	I_1	I_1	0.4676 (I_1)	0.2086 (I_7)	0.2590 (I_1–I_7)
2	−0.1173	0.0066	0.2546	−0.0711	−0.3930	0.0201	−0.0687	I_3	I_3	0.2546 (I_3)	0.0201 (I_6)	0.2345 (I_3–I_6)
3	0.3980	0.2353	0.1451	0.1705	−0.1473	−0.0508	0.1363	I_1	I_1	0.3980 (I_1)	0.2353 (I_2)	0.1627 (I_1–I_2)
4	0.0009	0.1891	0.3215	0.0690	−0.3425	0.1758	0.1410	I_3	I_3	0.3215 (I_3)	0.1891 (I_6)	0.1324 (I_3–I_6)
5	0.1154	0.7580	0.1074	0.0669	−0.2615	0.2103	0.0362	I_2	I_2	0.7580 (I_2)	0.2103 (I_6)	0.5477 (I_2–I_6)
6	0.0795	−0.1014	−0.2155	−0.1859	0.5255	−0.3736	−0.2489	I_5	I_5	0.5255 (I_5)	0.0795 (I_1)	0.4460 (I_5–I_1)
7	0.1326	0.7666	0.1340	0.0791	−0.2666	0.2106	0.0366	I_2	I_2	0.7666 (I_2)	0.2106 (I_1)	0.5560 (I_2–I_1)
8	0.2909	0.2987	0.2183	0.7536	−0.1159	−0.0170	0.6218	I_4	I_4	0.7536 (I_4)	0.6218 (I_7)	0.1318 (I_4–I_7)
9	−0.0141	0.4176	−0.0458	−0.0702	−0.3363	0.5495	−0.1060	I_6	I_6	0.5495 (I_6)	0.4176 (I_2)	0.1319 (I_6–I_2)
10	0.0723	−0.0960	−0.1990	−0.1718	0.6114	−0.3822	−0.2588	I_5	I_5	0.6114 (I_5)	0.0723 (I_1)	0.5391 (I_5–I_1)
11	0.1240	0.2187	0.0872	0.1703	−0.1581	−0.0089	0.6767	I_7	I_7	0.6767 (I_7)	0.2187 (I_2)	0.4580 (I_7–I_2)
12	0.2909	0.2986	0.2183	0.7548	−0.1159	−0.0170	0.6215	I_4	I_4	0.7548 (I_4)	0.6215 (I_7)	0.1333 (I_4–I_7)
13	−0.3081	−0.2864	−0.2473	−0.3343	−0.5392	0.1319	−0.3565	I_6	I_6	0.1319 (I_6)	−0.2473 (I_3)	0.3792 (I_6–I_3)
14	0.2719	0.2772	0.1907	0.2239	−0.1713	−0.0174	0.4975	I_7	I_7	0.4975 (I_7)	0.2772 (I_2)	0.2203 (I_7–I_2)

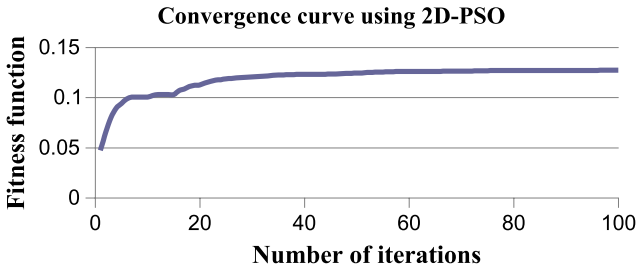

Fig. 2. Convergence characteristics of the proposed 2D-PSO method for $d\lambda_{set} = 0.132$.

the islanding categories with the fine-tuned weighting distributions $W_{p1} = 0.531$, $W_{p2} = 0.273$ and $W_{p3} = 0.196$. Fig. 2 shows the convergence characteristics of the proposed 2D-PSO method for the setting $d\lambda_{set} = 0.132$. The average number of iterations taken to reach the optimum solution is 46.2.

The minimum correlation value difference and average number of iterations obtained using the GA, EP, and 2D-PSO methods are summarized in Table 6, for comparison. It is clear from Table 6 that the correlation value difference obtained by the proposed method is larger as compared to those obtained by the GA and EP methods. However, the average number of iterations needed to reach the optimum solution is less.

To verify the performance of the proposed 2D-PSO extension islanding detection algorithm, a circuit based PSIM model of the grid-connected PV system shown in Fig. 1 is developed for simulation [20,21]. Fig. 3 shows when the grid power end has an islanding operation occurring at about the fourth second, while the system has experienced three periods of voltage

Table 6
Minimum correlation value difference and average number of iterations obtained using the GA, EP, and 2D-PSO methods.

Method	Average number of iterations	λ_p	λ_q	$min\{\lambda_p - \lambda_q\}$
GA	378.5	0.7531 (I_4)	0.6214 (I_7)	0.1317 (I_4–I_7)
EP	71.7	0.7528 (I_4)	0.6210 (I_7)	0.1318 (I_4–I_7)
2D-PSO	46.2	0.7536 (I_4)	0.6218 (I_7)	0.1318 (I_4–I_7)

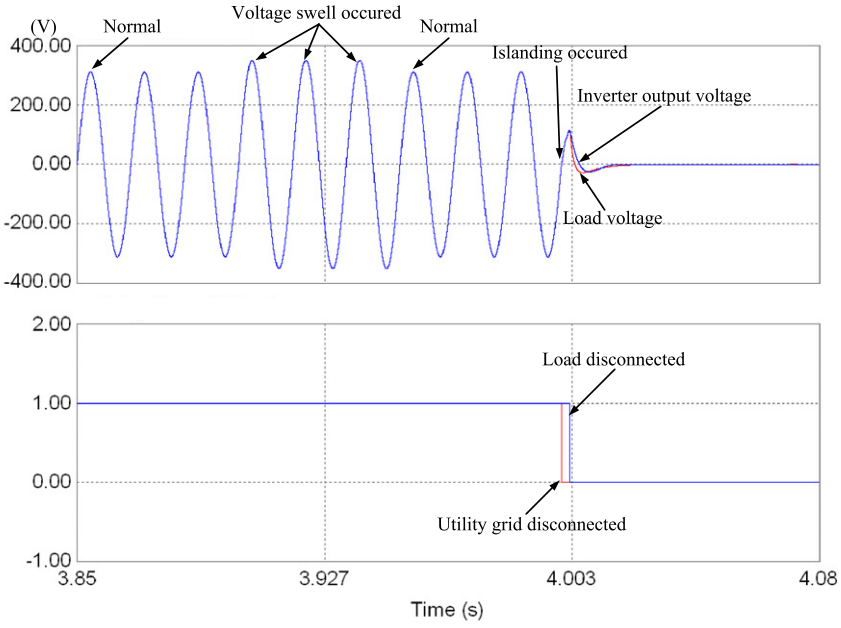

Fig. 3. Simulation results for the islanding operation detection when a voltage swell occurs.

swells (the amplitude of the applied grid voltage rises to 110% of the rated value); as seen, the 2D-PSO extension islanding detection method can distinguish a voltage swell arising from signal interference from an islanding phenomenon, and the load is not cut off up to a 0.5 period after the actual islanding occurrence. Fig. 4 shows the situation when a voltage dip (the amplitude of the applied grid voltage drops to 90% of the rated value) occurs in the grid-connected PV system and the grid power end also has an islanding operation at about the fourth second. As seen, the proposed method can definitely identify the voltage dip as electrical disturbance, and the load is cut off in a 0.5 period after the actual islanding operation. Fig. 5 shows the islanding operation detection when a voltage flicker occurs, which is formed by a 15 Hz and a 20 Hz flicker voltage and a 60 Hz standard voltage, and the actual islanding operation occurs at about the fourth second; the controller cut off the load in the 0.5 period later on in the islanding operation. Fig. 6 shows the simulation of a harmonic disturbance prior to an islanding operation, in order to allow us to observe whether islanding detection is influenced; the harmonic components added in are the third, fifth, and seventh harmonics, and the harmonic components are 10%, 7%, and 5%, respectively, of the fundamental frequency. As shown in Fig. 6, the system has an islanding operation at about the fourth second, and the proposed 2D-PSO extension islanding detection method does not result in a misjudgment, although the system was disturbed by harmonics prior to the islanding operation.

5. Conclusions

The proposed 2D-PSO method could help us to fine-tune the weighting for the correlation function in an extension method and obtain a better weighting in order to improve the islanding detection for PV power generation systems. The proposed 2D-PSO extension method is realized by combining the multi-variable detection methods of passive and active islanding detection. Power quality disturbances, such as voltage swells, voltage dips, power harmonics, and voltage flickers at the grid power end, are also analyzed in order to identify whether the abnormality at the grid power end is a power quality disturbance or an actual islanding operation. The simulated results showed that the proposed islanding detection method could detect islanding operations correctly and promptly cut the load from the photovoltaic power system within the set time, to match the IEEE Standards.

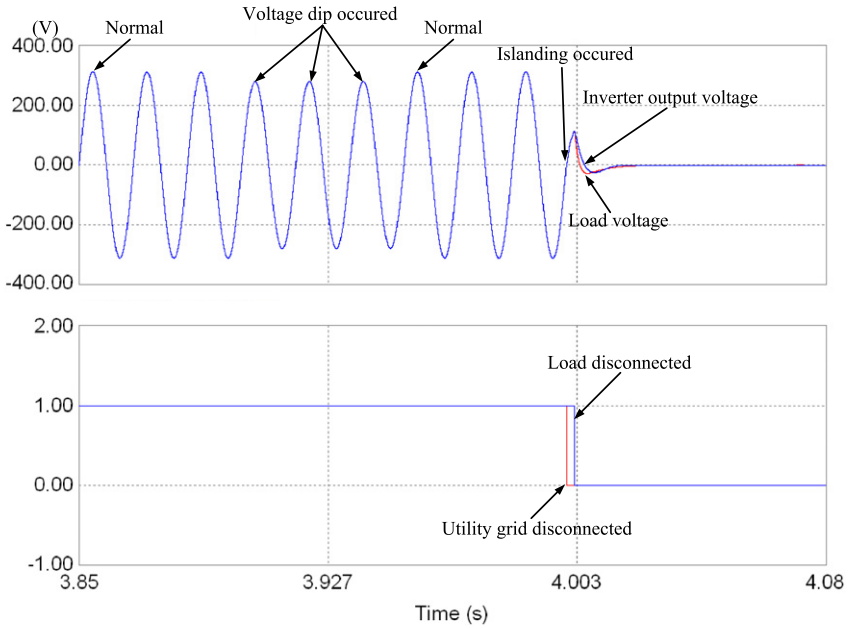

Fig. 4. Simulation results for the islanding operation detection when a voltage dip occurs.

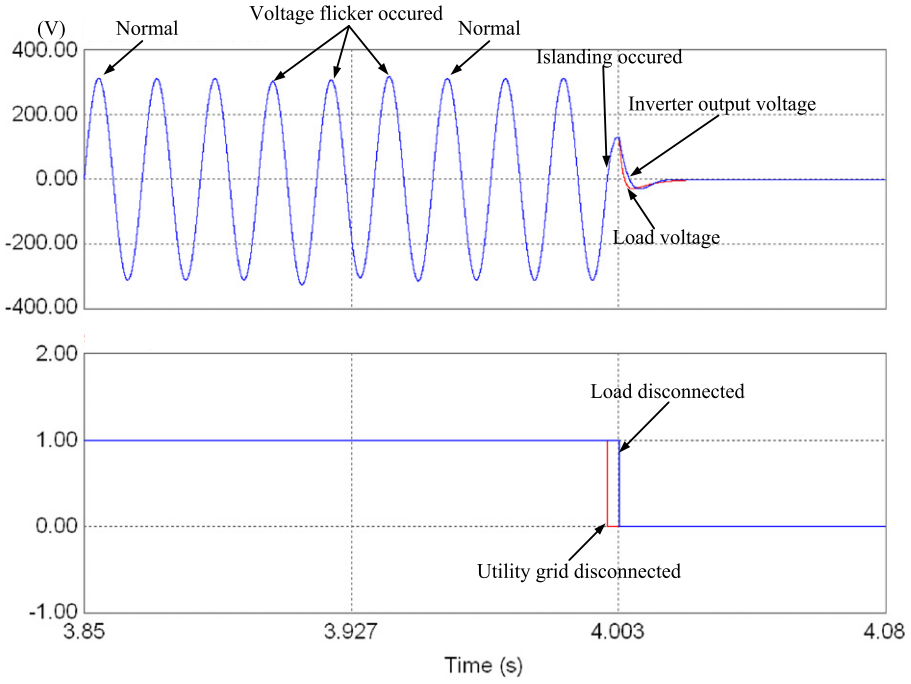

Fig. 5. Simulation results for the islanding operation detection when voltage flicker occurs.

Acknowledgment

The financial support of this research by the National Science Council of the R.O.C., under Grant No. NSC100-3113-E007-006, courtesy of the National Energy Technology Research Program, is greatly appreciated.

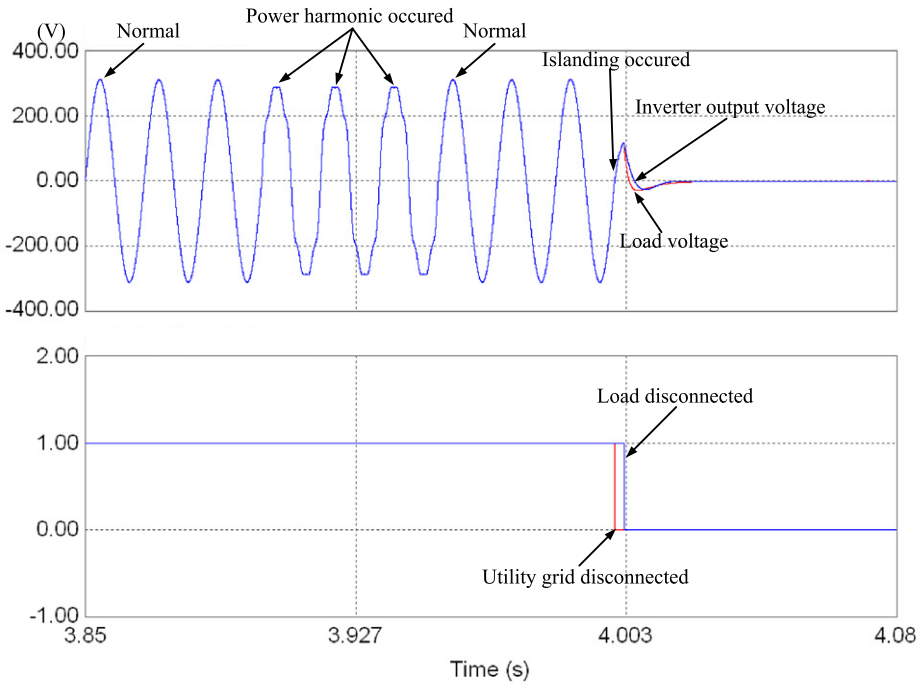

Fig. 6. Simulation results for the islanding operation detection when power harmonic occurs.

References

[1] F. De Mango, M. Liserre, A.D. Aquila, Overview of anti-islanding algorithms for PV systems. Part I: Passive methods, in: Proceeding of 12th Int. Power Electron. and Motion Control Conf., 2006, pp. 1878–1883.
[2] C. Jeraputra, P.N. Enjeti, Development of a robust anti-islanding algorithm for utility interconnection of distributed fuel cell powered generation, IEEE Transactions on Power Electronics 19 (5) (2004) 1163–1170.
[3] R.A. Jones, T.R. Sims, A.F. Imece, Investigation of potential island of self commutated static power converter in photovoltaic systems, IEEE Transactions on Energy Conversion 5 (4) (1990) 624–631.
[4] IEEE standard for interconnecting distributed resources with electric power systems, IEEE Std. 1547, 2003.
[5] G.A. Smith, P.A. Onions, D.G. Infield, Predicting islanding operation of grid connected PV inverters, IEE Proceeding: Electric Power Applications 147 (1) (2000) 1–6.
[6] L.A.C. Lopes, H. Sun, Performance assessment of active frequency drifting islanding detection methods, IEEE Transactions on Energy Conversion 21 (1) (2006) 171–180.
[7] V. John, Z. Ye, A. Kolwalkar, Investigation of anti-islanding protection of power converter based distributed generators using frequency domain analysis, IEEE Transactions on Power Electronics 19 (5) (2004) 1177–1183.
[8] Z. Ye, L. Li, L. Garces, C. Wang, R. Zhang, M. Dame, R. Walling, N. Miller, A new family of active anti-islanding schemes based on DQ implementation for grid-connected inverters, in: Proceeding of 35th Annu. IEEE Power Electron. Speci. Conf., 2004, pp. 235–241.
[9] K.H. Chao, C.L. Chiu, An intelligent islanding detection method based on extension theory for photovoltaic power generation systems, in: Proceeding of the International Symposium on Computer. Communication, Control and Automation, 3CA2010, 2010, pp. 171–174.
[10] J. Kołodziej, F. Xhafa, Integration of task abortion and security requirements in GA-based meta-heuristics for independent batch grid scheduling, Computers & Mathematics with Applications 63 (2) (2012) 350–364.
[11] G. Chiandussi, M. Codegone, S. Ferrero, F.E. Varesio, Comparison of multi-objective optimization methodologies for engineering applications, Computers & Mathematics with Applications 63 (5) (2012) 912–942.
[12] J. Kennedy, R. Eberhart, Particle swarm optimization, in: Proceeding of IEEE International Conf. on Neural Networks, 1995, pp. 1942–1948.
[13] R.C. Eberhart, J. Kennedy, A new optimizer using particle swarm theory, in: Proceeding of the 6th International Symposium on Micromachine and Human Science, 1995, pp. 39–43.
[14] J. Mádar, J. Abonyi, F. Szeifert, Interactive particle swarm optimization, in: Proceeding of ISDA, 2005, pp. 314–319.
[15] M. Jaberipour, E. Khorram, B. Karimi, Particle swarm algorithm for solving systems of nonlinear equations, Computers & Mathematics with Applications 62 (2) (2011) 566–576.
[16] X. Chao, Y.J. Li, K. Zhang, L. Wang, Shadow detecting using particle swarm optimization and the Kolmogorov test, Computers & Mathematics with Applications 62 (7) (2011) 2704–2711.
[17] W. Cai, The extension set and incompatibility problem, Journal of Scientific Exploration 1 (1983) 81–93.
[18] Y.P. Huang, S.W. Chiou, L.C. Liou, Extension Engineering Methods, first ed., Chuan Hwa Book Corporation, Taiwan, 2001.
[19] Kyocera Photovoltaic Module KC40T Specifications, Kyocera Solar Industries.
[20] PSIM User's Guide, Powersim Inc., 2001, 2003.
[21] K.H. Chao, S.H. Ho, M.H. Wang, Modeling and fault diagnosis of a photovoltaic system, Electric Power Systems Research 78 (1) (2008) 97–105.